Crystal symmetry and high-magnetic-field specific heat of $SrCu_2(BO_3)_2$

G. A. Jorge,[1,*] R. Stern,[2] M. Jaime,[1] N. Harrison,[1] J. Bonča,[3,4] S. El Shawish,[4] C. D. Batista,[5] H. A. Dabkowska,[6] and B. D. Gaulin[6]

[1]*MST-NHMFL, Los Alamos National Laboratory, Los Alamos, New Mexico 87545, USA*
[2]*National Institute of Chemical Physics and Biophysics (NICPB), Tallinn, Estonia*
[3]*Department of Physics, FMF University of Ljubljana, 1000 Ljubljana, Slovenia*
[4]*J. Stefan Institute, 1000 Ljubljana, Slovenia*
[5]*Theoretical Division, Los Alamos National Laboratory, Los Alamos, New Mexico 87545, USA*
[6]*Department of Physics and Astronomy, McMaster University, Hamilton, ON, Canada L8S 4C6*

(Received 4 October 2004; revised manuscript received 19 November 2004; published 23 March 2005)

We report measurements of the specific heat of the quantum spin liquid system $SrCu_2(BO_3)_2$ in continuous magnetic fields H of up to 33 T. The specific heat data, when combined with a finite temperature Lanczos diagonalization of the Shastry-Sutherland Hamiltonian, indicate the presence of a nearest neighbor Dzyaloshinsky-Moriya (DM) interaction that violates the crystal symmetry. Moreover, the same DM interaction is required to explain the observed electron spin resonance lines for $H \| c$.

DOI: 10.1103/PhysRevB.71.092403 PACS number(s): 75.45.+j, 05.30.Jp, 67.40.Db, 75.40.Cx

$SrCu_2(BO_3)_2$ is a quasi-two dimensional spin system with a singlet dimer ground state.[1] It is the only known realization of the Shastry-Sutherland model,[2] and exhibits a sequence of magnetization plateaux at high magnetic fields H.[3,4] The unique behavior of this quantum spin liquid results from the interplay between two different fascinating aspects of strongly correlated spin systems: namely *geometrical frustration* and *strong quantum fluctuations*. The spin $s=1/2$ Cu^{2+} ions that are responsible for the magnetism are grouped in dimers within planes of the tetragonal $SrCu_2(BO_3)_2$ unit cell, with respective intradimer or nearest neighbor (nn) and interdimer or next nearest neighbor (nnn) separations of 2.9 and 5.1 Å. The coupling constants are estimated to be $J \sim 80$ K for nn and $J' \sim 50$ K for nnn.[5] The geometrical frustration of the spin lattice leads to very localized triplet excitations that have a tendency to crystallize at high H. This occurs when the concentration of triplets reaches certain values that are commensurate with the underlying lattice, becoming incompressible upon formation of a gapped structure. The magnetization plateaux at $H_{p1}=27$ T, $H_{p2}=35$ T, and $H_{p3}=42$ T, observed when H is applied along the crystallographic tetragonal c axis, are a direct consequence of spin superstructures forming at triplet concentrations 1/8, 1/4, and 1/3, respectively.[6]

Recent electronic spin resonance (ESR) experiments[7–9] reveal spin triplet excitation lines of energy ~ 3 meV that split for finite H. The two lower energy branches decrease linearly with increasing $H \| c$, and extrapolate to zero around $H=22$ T. On approaching 22 T, the ESR data deviate from this linear extrapolation, indicating a level anticrossing between the first triplet excitation and the ground state. These finite ESR lines are not allowed by the known crystal symmetry space group $I\bar{4}2m$.[10,11] Moreover, the anticrossing implies some mixing between two states with different magnetization M_z along the tetragonal c axis. This observation cannot be explained by the $U(1)$ invariant models (which are symmetric under rotations around the c axis) proposed in previous works, for which M_z is a good quantum number.

In this report, we show that an interaction which breaks the known crystal symmetry is required to reproduce the ESR data,[7–9] and also explains the low temperature specific heat $[C(T)]$ for $H \gtrsim 18$ T. This minimal extension of the model Hamiltonian[11] consists of only one additional parameter, the z-component D_z (along the c axis) of the nearest-neighbor Dzyaloshinsky-Moriya (DM) interaction. This component mixes each singlet dimer state with the $S_z=0$ triplet component enabling transitions between the ground state and $S_z=\pm 1$ triplet excitations. The structural distortion could be driven by strong spin-lattice interactions that would be a relevant ingredient to explain the details of the magnetization plateaux observed in this system.

The single crystal sample of $SrCu_2(BO_3)_2$ used in this study was grown by the floating zone technique. Stoichiometric amounts of CuO, $SrCO_3$, and B_2O_3 were mixed, preannealed, and then annealed at 870 °C. Finally, the powder was regrinded, pelletized, and annealed in O_2 several times. Rods were formed by hydrostatic pressing and the growth was performed in a Crystal System Optical Furnace at a growth speed of 0.25 mm/h in O_2. No additional flux was applied.[12] The measurements of $C(T,H)$ of $SrCu_2(BO_3)_2$ in continuous magnetic fields up to 33 T were performed on two oriented single crystal pieces of 12.34 and 13.92 mg. Both were measured with H applied along the tetragonal c axis and within the ab planes. A calorimeter made of plastic materials and silicon was used, employing a thermal relaxation time technique optimized for rapid data acquisition.[13,14] The magnetization $M_z(H)$ of a piece of sample of approximate dimensions $1.5 \times 0.9 \times 0.5$ mm^3 was measured using a sample-extraction magnetometer in a 400 ms, 45 T pulsed magnet provided by the National High Magnetic Field Laboratory at Los Alamos.[15] The small size of the sample, placed in good thermal contact with liquid ^{3}He or ^{4}He below $T=4$ K, combined with the relatively slow field sweep of the magnet helped minimize magnetocaloric effects so as to achieve an isothermal experiment.[16] For characterization purposes, supplementary $M_z(T)$ measurements and $C(T,H)$

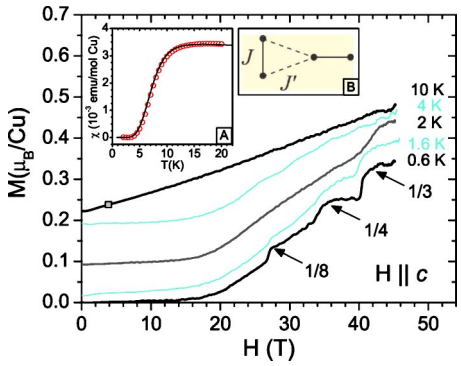

FIG. 1. (Color online) Magnetization vs field for $SrCu_2(BO_3)_2$ at different temperatures between 0.6 and 10 K, as indicated, reveal a gradual evolution of the magnetization plateaux. The square point on the 10 K curve was used to compare with SQUID magnetometer data in order to obtain the magnetization units. Inset (a) Magnetic susceptibility measured at $H=4$ T in a SQUID magnetometer (circles). The solid line is the susceptibility calculated with the FTL method. Inset (b) Two copper dimers in the $CuBO_3$ plane where the coupling constants J (nn) and J' (nnn) are indicated.

measurements were made at lower fields using a commercial Quantum Design™ MPMS [superconducting quantum interference device (SQUID) magnetometer]. Meanwhile, numerical simulations of the Shastry-Sutherland model, with which the experimental data are compared, were performed on a 20-site square lattice using the finite T Lanczos (FTL) method.[17–19]

To describe the present system, we consider the following Heisenberg Hamiltonian on a Shastry-Sutherland lattice:[2]

$$H_s = J\sum_{\langle \mathbf{i},\mathbf{j}\rangle} \mathbf{S_i}\cdot\mathbf{S_j} + J'\sum_{\langle \mathbf{i},\mathbf{j}\rangle'} \mathbf{S_i}\cdot\mathbf{S_j} + \sum_{\langle \mathbf{i}\rightarrow\mathbf{j}\rangle} \mathbf{D}\cdot(\mathbf{S_i}\times\mathbf{S_j}) + \sum_{\langle \mathbf{i}\rightarrow\mathbf{j}\rangle'} \mathbf{D}'\cdot(\mathbf{S_i}\times\mathbf{S_j}). \quad (1)$$

Here, $\langle i,j\rangle$ and $\langle i,j\rangle'$ indicate that $\mathbf{i}$ and $\mathbf{j}$ are nn and nnn, respectively. The Hamiltonian includes nn ($\mathbf{D}$) and nnn ($\mathbf{D}'$) DM interactions.[20,21] The arrows indicate that the corresponding bonds have a particular orientation.[7,22] The quantization axis $\hat{\mathbf{z}}$ is parallel to the c axis. According to the crystal symmetry space group $I\bar{4}2m$, the xy component of $\mathbf{D}$ must be perpendicular to the corresponding dimer and $D_z=0$. However, we find that a nonzero z component of $\mathbf{D}$, not allowed by the space group, can explain *simultaneously* $C(T)$ and the ESR data as a function of H. Relaxing the condition on the xy component alone, on the other hand, is not supported by experimental data since it does not lead to finite ESR lines for $H\|c$. The nnn DM interaction[11] is required to account for the spliting between the two single triplet excitations.[7,9,23,24] From the observed splitting between the two lowest triplet excitations in an applied field $H\|c$, D'_z is estimated to be 2.1 K.[7] The much smaller splitting observed when $H\|a$, indicates that D'_x and D'_y can be neglected for all practical purposes.

Figure 1 shows $M_z(H)$ measured as a function of H, in units of μ_B/Cu determined upon crosscalibration with

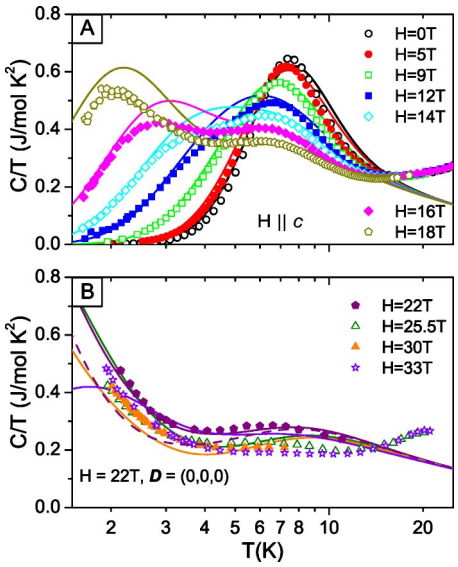

FIG. 2. (Color online) Measured specific heat divided by T (symbols) vs T compared with the calculated one for the Hamiltonian of Eq. (1) (solid lines) for the magnetic field along the c axis: (a) $0\leqslant H\leqslant 18$ T and (b) $20\leqslant H\leqslant 33$ T. The parameters are the same ones used to compute the magnetic susceptibility. The dashed line is the calculated C/T for $\mathbf{D}=0$ and $H=22$ T.

SQUID magnetometry data. In addition to the plateaux already mentioned, there is a small excess contribution to M_z identified in our data over the entire field range. This additional source of magnetization has been observed before in SQUID magnetometry data.[3] For our samples, both SQUID magnetometry data and low field pulsed magnetic field data evidence a finite excess susceptibility of approximately 0.115×10^{-3} emu/mol Cu, probably due to crystalline defects. Good agreement with the expected magnetization values at the plateaux is obtained by subtracting this value. Better agreement is obtained by subtracting a scaled Brillouin function with an initial slope of 0.14×10^{-3} emu/mol Cu and a characteristic temperature of 5 K (see Fig. 1). After either of these substractions, there remains a finite value of M_z at very low temperatures and magnetic fields that increases linearly with H.

In the inset of Fig. 1 we compare the measured magnetic susceptibility $\chi(T)$ (after subtracting a small constant value of 0.14×10^{-3} emu/mol Cu) and the curve obtained with the FTL method that is described below. We get an excellent agreement for: $J=74$ K, $J'=0.62J$, $\mathbf{D}=(2.2\text{ K},\pm2.2\text{ K},5.2\text{ K})$ (the sign is different for each dimer in the unit cell), $\mathbf{D}'=(0,0,2.2\text{ K})$. The values of the g factors, $g_\parallel=2.15$ and $g_\perp=2.08$, have been obtained from a comparison between our theoretical calculations[25] (see Fig. 4) and the ESR spectra.[7,9]

In Fig. 2, we show $C(T,H)/T$ for different values of H applied along the c axis. The primary feature in the low T specific heat is a broad anomaly centered at $T=8.5$ K that is gradually depressed by increasing H. This anomaly has been attributed[26] to $S_z=0$ dimer excitations. Here, however, we observe a small shift in T as function of H indicating the involvement of states with $S_z\neq0$. For $H\geqslant12$ T, a second

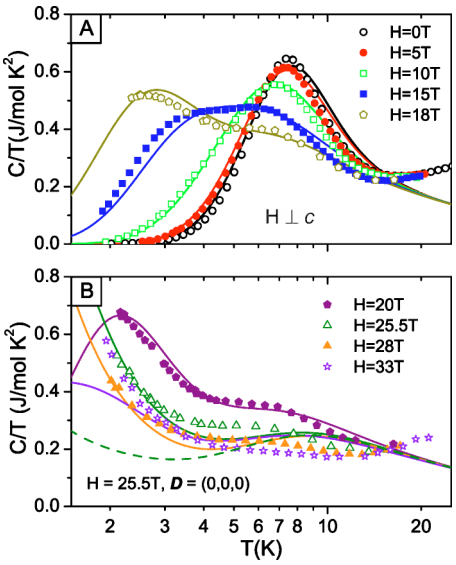

FIG. 3. (Color online) Measured specific heat divided by T (symbols) vs T compared with the calculated one for the Hamiltonian of Eq. (1) (solid lines) for the magnetic field perpendicular to the c axis: (a) $0 \leqslant H \leqslant 18$ T and (b) $22 \leqslant H \leqslant 33$ T. The parameters are the same ones used to compute the magnetic susceptibility. The dashed line is the calculated C/T for $\mathbf{D}=0$ and $H=25.5$ T.

anomaly develops at lower T, which we attribute to $S_z=1$ excitations situated 3 meV above the ground state in zero field. The Zeeman interaction causes this triplet state to move to lower energies with increasing H. Figure 3 shows similar results for $H \perp c$.

In Figs. 2 and 3, we also compare the experimental results with the results of a numerical simulation of $C(T,H)/T$ made using the FTL method.[17,18] This method is based on the Lanczos procedure of exact diagonalization, and uses a random sampling over initial wave functions specially adapted for calculation of thermodynamic properties. All the results were computed on a tilted square lattice of $N=20$ sites. There are many advantages of this method over the conventional Quantum Monte Carlo (QMC) simulations, which are as follows: first, the minus-sign problem that usually appears in QMC calculations of frustrated spin systems is absent; second, the method connects the high and low-temperature regimes in a continuous fashion, enabling the entropy density and specific heat (per unit cell) to be computed as expectation values (i.e., $s=k_B \ln Z/N+\langle H\rangle/NT$, where Z is the statistical sum). The specific heat is then given by $C_V=T(\partial s/\partial T)=k_B(\langle H^2\rangle-\langle H\rangle^2)/NT^2$. The main limitation to the validity of the results originates from finite-size effects which occur when $T<T_{fs}$. The actual value of T_{fs} depends strongly on the particular physical properties of the system. For gapless systems, T_{fs} can be defined by way of the thermodynamic sum $\overline{Z}(T)=\mathrm{Tr}\exp[-(H-E_0)/T]$, on condition that $\overline{Z}(T_{fs})=Z^* \gg 1$.[18] In the present case, this condition can be relaxed ($Z^*>1$) owing to the existence of a gap in the excitation spectrum when $J'/J<0.7$ and to the almost localized nature of the lowest excited states—triplet excitations. By comparing results obtained on two different systems with $N=16$ and $N=20$ sites, we estimate $T_{fs}<1$ K.

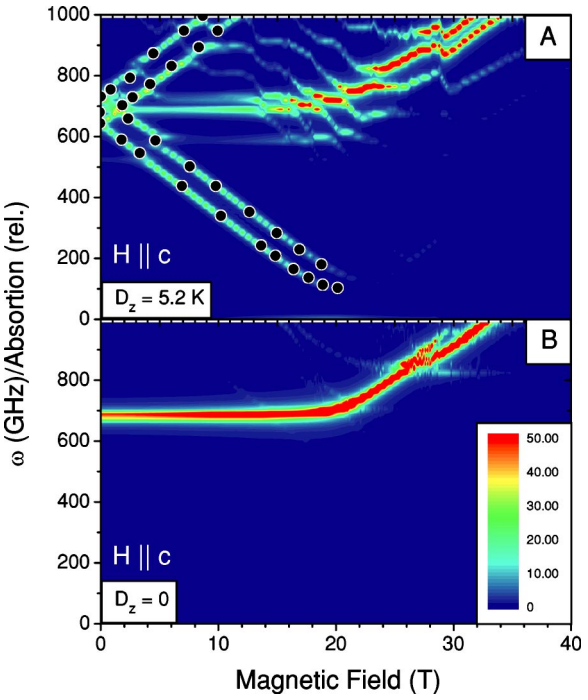

FIG. 4. (Color online) Contour color plot for the ESR spectrum for $H \| c$ calculated with the Lanczos method in a 20 sites cluster for (a) $D_z=5.2$ K and (b) $D_z=0$. The values of the other parameters are the same ones used to compute the magnetic susceptibility. The experimental data points in (a) are from Cepas *et al.* (See Ref. 6).

For $H<18$ T, the agreement between theory and experiment is very good, regardless of the inclusion of D_z. Finite size effects are also very small due to the localized nature of the single-triplet excitations.[24] However, when H approaches 22 T for $H \| c$ (or 25 T for $H \perp c$), the inclusion of this interaction explains the measured $C(T,H)/T$ at low temperatures. For $H \| c$, this is explained by the fact that D_x and D_y are the only interactions that violate the conservation of M_z, by mixing the $M_z=0$ ground state of the Hamiltonian $H_s(\mathbf{D}=0)$ with the single-triplet excited state with $M_z=\pm 1$. This mixing becomes effective only when the energy difference between both levels is comparable to $|\mathbf{D}|$. For $H \perp c$, the same type of mixing is produced by the z component of $\mathbf{D}$. In other words, the level crossing that would occur if $D_z=0$ is replaced by level anticrossing. This can be seen in Figs. 2(b) and 3(b) where we also show the calculated C/T for $\mathbf{D}=0$ and $H=22$ T ($H=25.5$ T) for $H \| c$ ($H \perp c$). In absence of the component D_z, the level crossing generates a peak of C/T at $T=0$ which is not consistent with the experiment. In contrast, the level anticrossing moves this peak to higher temperatures in agreement with the experimental data. The anticrossing occurs for different values of H in the different field orientations due to the anisotropy of the g factor.[7,9] At high temperatures ($T>20$ K), the specific heat data deviates from the theoretical prediction owing to significant phonon contributions. For $T \sim 10$ K and fields $H>20$ T, there are small deviations between the experimental curves and the calculations, which can be attributed to the inter planar antiferromagnetic interaction $J''/J \sim 0.21$ that becomes relevant when the concentration of triplet dimer states increases.

The proposed nonzero D_z is further supported by the measured ESR spectrum for $H\|c$.[7,9] In Fig. 4, we show the ESR spectrum as a function of H for $D_z=5.2$ K [Fig. 4(a)] and $D_z=0$ K [Fig. 4(b)] calculated with the Lanczos method.[25] More specifically, we are computing the dynamical susceptibility along the direction perpendicular to the applied field using the method introduced in Ref. 27. As it is pointed out in Ref. 8, the observed ESR trasitions between the ground state and the single-triplet excitations for $H\|c$ are not allowed by the observed space symmetry group $I\bar{4}2m$.[10] We show that these ESR transitions can be explained with a nonzero value of D_z, while the corresponding ESR lines are not present if $D_z=0$ [Fig. 4(b)]. None of the other components of $\mathbf{D}$ or $\mathbf{D}'$ can reproduce these ESR lines. Based on these observations, we propose that the crystal symmetry is lowered at low temepratures due to a strong spin-lattice interaction. Since the lattice distortion depends on the applied field, we expect D_z to be an increasing function of H (although we used a constant value $D_z=5.2$ K for our calculation). Ultrasonic experiments[28] indicate that in this region the lattice is coupled to the magnetic field.

With the exception of D_z, all other physical parameters used in the model were determined from previous experiments. The values of $g_\parallel$ and $g_\perp$ are obtained from the ESR spectra.[7,9] By including a finite D_z, however, we are able to account simultaneously for the ESR spectra as a function of the applied field (see also Ref. 25), the low temperature specific heat data for $H\gtrsim 18$ T, and the temperature dependence of the susceptibility.

In summary, we have measured the specific heat as a function of temperature in continuous magnetic fields up to 33 T. An excellent fit to the $C(T,H)/T$ data for both field orientations is obtained for a nn exchange constant $J=74$ K, a ratio $J'/J=0.62$, a nn Dzyaloshinsky-Moriya interaction constant $|\mathbf{D}|=6.1$ K, and a nnn Dzyaloshinsky-Moriya interaction constant $|\mathbf{D}'|=2.2$ K. A nonzero value of D_z, that is not allowed by the observed crystal symmetry, can explain both the specific heat data for $H\gtrsim 18$ T and the observed ESR[7,9] spectrum for $H\|c$. This suggests that a lattice distortion that lowers the crystal symmetry is induced at low temperatures. A more detailed comparison between the calculated ESR spectrum and the experiment will be presented elsewhere.[25]

This work was sponsored by the US DOE under Contract No. W-7405-ENG-36. R.S. was supported by the National High Magnetic Field Laboratory and Estonian Science Foundation Grant No. 4931. J.B. acknowledges the financial support of Slovene MESS. Work performed at the National High Magnetic Field Laboratory is supported by the National Science Foundation (DMR90-16241), the Department of Energy and the State of Florida.

*Also at: Departamento de Física, Universidad de Buenos Aires, Bs. As., Argentina.

[1] R. W. Smith and D. A. Kesler, J. Solid State Chem. **93**, 430 (1991).

[2] B. S. Shastry and B. Sutherland, Physica B & C **108B**, 1069 (1981).

[3] H. Kageyama *et al.*, Phys. Rev. Lett. **82**, 3168 (1999).

[4] K. Onizuka, H. Kageyama, Y. Narumi, K. Kindo, Y. Ueda, and T. Goto, J. Phys. Soc. Jpn. **69**, 1016 (2000).

[5] S. Miyahara and K. Ueda, Phys. Rev. Lett. **82**, 3701 (1999).

[6] K. Kodama *et al.*, Science **298**, 395 (2002).

[7] O. Cépas *et al.*, Phys. Rev. Lett. **87**, 167205 (2001).

[8] O. Cépas and T. Ziman, Phys. Rev. B **70**, 024404 (2004).

[9] H. Nojiri, H. Kageyama, Y. Ueda, and M. Motokawa, J. Phys. Soc. Jpn. **72**, 3243 (2003).

[10] K. Sparta *et al.*, Eur. Phys. J. B **19**, 507 (2001).

[11] S. Miyahara and K. Ueda, J. Phys.: Condens. Matter **15**, R327 (2003).

[12] H. Dabkowska and B. D. Gaulin (unpublished).

[13] M. Jaime *et al.*, Nature (London) **405**, 160 (2000).

[14] G. A. Jorge, Tesis Doctoral, Universidad de Buenos Aires, 2004.

[15] G. A. Jorge, M. Jaime, N. Harrison, R. Stern, H. Dabkowska, and B. D. Gaulin, J. Alloys Compd. **369**, 90 (2004).

[16] M. Jaime, K. H. Kim, G. A. Jorge, S. McCall, and J. A. Mydosh, Phys. Rev. Lett. **89**, 287201 (2002).

[17] J. Jaklič and P. Prelovšek, Phys. Rev. Lett. **77**, 892 (1996); Phys. Rev. B **49**, 5065 (1994).

[18] J. Jaklič and P. Prelovšek, Adv. Phys. **49**, 1 (2000).

[19] J. Bonča and P. Prelovšek, Phys. Rev. B **67**, 085103 (2002).

[20] I. Dzyaloshinski, J. Phys. Chem. Solids **4**, 241 (1958).

[21] T. Moriya, Phys. Rev. **120**, 91 (1960).

[22] A. Zorko, D. Aron, H. van Tol, L. C. Brunel, and H. Kageyama, Phys. Rev. B **69**, 174420 (2004).

[23] T. Rõõm U. Nagel, E. Lippmaa, H. Kageyama, K. Onizuka, and Y. Ueda, Phys. Rev. B **61**, 14 342 (2000).

[24] H. Kageyama *et al.*, Phys. Rev. Lett. **84**, 5876 (2000).

[25] S. El Shawish, J. Bonča, C. D. Batista, I. Sega, cond-mat/0407632 (unpublished).

[26] M. Hofmann T. Lorenz, G. S. Uhrig, H. Kierspel, O. Zabara, A. Freimuth, H. Kageyama, and Y. Ueda, Phys. Rev. Lett. **87**, 047202 (2001).

[27] E. R. Gagliano and C. A. Balseiro, Phys. Rev. Lett. **59**, 2999 (1987).

[28] S. Zherlitsyn *et al.*, Phys. Rev. B **62**, R6097 (2000).